PHYSICAL REVIEW B **79**, 100106(R) (2009)

Synthesis and characterization of multiferroic $BiMn_7O_{12}$

F. Mezzadri,[1,*] G. Calestani,[1,2] M. Calicchio,[2] E. Gilioli,[2] F. Bolzoni,[2] R. Cabassi,[2] M. Marezio,[3] and A. Migliori[4]
[1]*Dipartimento di Chimica GIAF, Università di Parma, Viale G.P. Usberti 17A, 43100 Parma, Italy*
[2]*Istituto dei Materiali per Elettronica e Magnetismo (IMEM), CNR, Area delle Scienze, 43100 Parma, Italy*
[3]*CRETA CNRS, 38042 Grenoble Cedex 9, France*
[4]*CNR-IMM, Via Gobetti 101, 40126 Bologna, Italy*
(Received 3 December 2008; published 20 March 2009)

We report on the high-pressure synthesis of $BiMn_7O_{12}$, a manganite displaying a "quadruple-perovskite" structure. Structural characterization of single-crystal samples shows a distorted and asymmetrical coordination around the Bi atom due to presence of the $6s^2$ lone pair, resulting in noncentrosymmetric space group *Im*, leading to a permanent electrical dipole moment and ferroelectric properties. On the other hand, magnetic characterization reveals antiferromagnetic transitions in agreement with the isostructural compounds, and the dielectric constant shows anomalies matching the magnetic transition temperatures. $BiMn_7O_{12}$ is therefore a promising multiferroic material, with evidence of coupling between magnetic and dielectric properties.

DOI: 10.1103/PhysRevB.79.100106 PACS number(s): 61.05.cp, 61.05.jm, 75.30.−m, 75.47.Lx

Multiferroics are defined as materials that simultaneously exhibit more than one ferroic order parameter among magnetic, electric, and elastic.[1] Although there are a lot of compounds presenting magnetic or ferroelectric order, the constrains required for their coexistence are so severe that only an extremely limited number of multiferroic materials exists. Besides scientific interest in their physical properties, multiferroics have potential for technological applications as actuators, switches, magnetic field sensors, or electronic memory devices. However, at present, only magnetoelectric composites, realized by combining magnetostrictive and piezoelectric materials, are ready for technological applications.[2] Typical multiferroics include rare-earth manganites and ferrites [$TbMnO_3$,[3] $HoMn_2O_5$,[4] and $LuFe_2O_4$ (Ref. 5)], bismuth-based compound $BiFeO_3$,[6] fluorides [$BaNiF_4$ (Ref. 7)] and spinel chalcogenides [$ZnCr_2Se_4$ (Ref. 8)]. In usual perovskite-based materials, the ferroelectric distortion occurs due to the displacement of *B*-site cation [for example, Ti in $BaTiO_3$ (Ref. 9)] with respect to the oxygen octahedral coordination. One possible mechanism for the coexistence of ferroelectricity and magnetism in perovskites is the presence in the *A* site of an atom carrying a nonbonding pair of electrons in an outer shell (lone pair), whose stereochemical effect may be at the origin of ferroelectricity. Examples include $BiFeO_3$ (Ref. 6) and $PbVO_3$.[10] On the other hand magnetic behavior is usually induced by partially filled *d* orbitals on the *B* site.

Following this idea we synthesized $BiMn_7O_{12}$, a compound belonging to the family of quadruple-perovskite ("quadruple" refers to the formula unit ABO_3) manganites, with general formula $AA'_3B_4O_{12}$,[11,12] derived by the doubling of the conventional ABO_3 manganites axes [Fig. 1(a)]. The complex and highly distorted structure is based on a three-dimensional network of corner-sharing MnO_6 tilted octahedra, centered on the *B* site, which makes $BiMn_7O_{12}$ a metastable material: it can only be accommodated under high pressure by the presence of a Jahn-Teller atom (Mn^{3+} or Cu^{2+}) on the *A'* site, displaying an uncommon square planar coordination due to large distortion of the standard dodecahedral coordination, typical of the *A* site. Since the occupation of the *A* site determines the properties of the compounds, the motivation of this work is the synthesis of the Bi-substitute member and to correlate the structural distortion induced by the Bi^{3+} lone pair to the electronic properties, in particular searching for multiferroicity.

$BiMn_7O_{12}$ was synthesized by solid-state reaction in high-pressure/high-temperature (HP/HT) conditions. Stoichiometric mixture of Mn_2O_3 (Ventron 98%) and Bi_2O_3 (Merck 99%) was used as reagent. They were mixed, finely grounded in glove box, and encapsulated in a Pt foil inserted in the MgO octahedral cell and in the multianvil apparatus. The pressure was increased up to its maximum value at a rate of 160 bar/min, then the capsule was heated up to the reaction temperature at a rate of 50 °C/min. The optimal conditions for the synthesis of a mixture of bulk material and single crystals were identified as 40 Kbar and 1000 °C. After 2 h in these conditions the sample was cooled down to room temperature by switching off the heater. The pressure was finally slowly released at 0.4 bar/min.

The crystal structure of $BiMn_7O_{12}$ at room temperature was determined by single-crystal x-ray diffraction (XRD). Intensity data were collected by using MoK_a data in the range of $3.79 \leq \theta \leq 28.83°$ on a Bruker AXS Smart diffractometer, equipped with a charge couple device (CCD) area detector. The structure is monoclinic, with lattice parameters $a=7.5351(15)$, $b=7.3840(15)$, $c=7.5178(15)$Å, and $\beta=91.225(3)°$. The cell volume is $V=418.19(15)$Å^3, consistent with 2 f.u./cell. In analogy with other monoclinic AMn_7O_{12} compounds,[13,14] the structure was initially refined with SHELX97 (Ref. 15) in the centrosymmetric space group $I2/m$, using anisotropic atomic displacements parameters (a.d.p.'s) for all the atoms. The refinement converged to $R_1=0.0535$, $wR_2=0.1413$, and goodness of fit (g.o.f.) =1.101 for 562 data and 59 parameters. In spite of the fact that these final agreement indices can be considered satisfactory, when the sole numeric values are considered, a careful inspection of the refined parameters points out a very unusual trend of the a.d.p.'s showing, in particular for the oxygen atoms, not only very high values but also an anomalous elongation in a common direction of the *ac* plane [Fig. 1(b)], which indicates static disorder. Therefore the possibility of an artifact

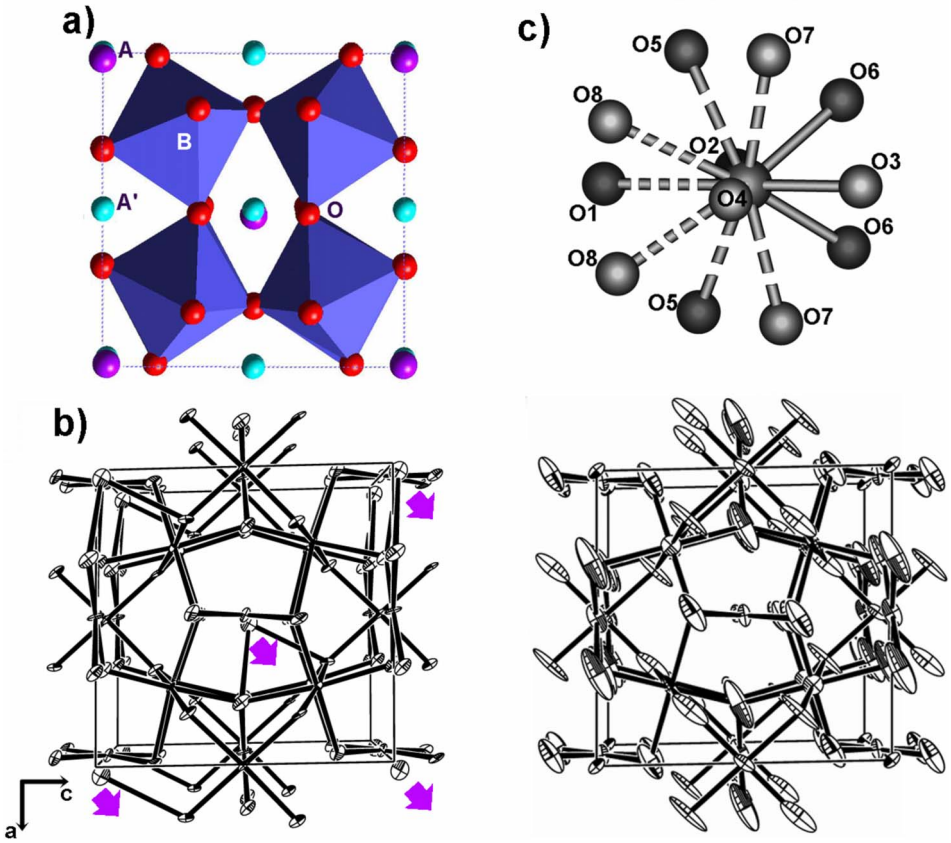

FIG. 1. (Color online) (a) $BiMn_7O_{12}$ cell viewed along the [001] direction. The site definition corresponds to the general formula $AA'_3B_4O_{12}$. (b) ORTEP perspective view of the $BiMn_7O_{12}$ structure refined in *Im* (left) and $I2/m$ (right) space groups. Displacement ellipsoids are drawn in both cases at the 50% probability level. The arrows in the left panel point out the Bi displacement direction. (c) Distorted dodecahedral coordination around the Bi atom in $BiMn_7O_{12}$; the weakest interactions are indicated by dashed bonds.

induced by forcing an acentric structure in a centric symmetry was considered and the structure was further refined in the noncentrosymmetric *I*2 and *Im* space groups, taking into account the possible occurrence of polar domains by twin refinement. While the results obtained in *I*2 are comparable to those of the centrosymmetric model, the ones produced in *Im* are characterized by a significant improvement in terms of agreement indices (R_1=0.0391, wR_2=0.0928, and g.o.f =1.113 for 1082 data and 103 parameters) and a.d.p.'s. The latter is clearly evidenced in Fig. 1(b), which shows a comparison of the ORTEP (Ref. 16) plots of the crystal structure of $BiMn_7O_{12}$ refined in both *Im* and $I2/m$ in which the a.d.p.'s are represented by ellipsoids drawn at the 50% probability level. Atomic parameters, refined in the acentric space group *Im*, and relevant bond distances are shown in Tables I and II, respectively. Charge distribution analysis, performed with

TABLE I. Atomic coordinates and displacement parameters for $BiMn_7O_{12}$. The isotropic displacement parameter U_{eq} is defined as one-third of the trace of the orthogonalized U_{ij} tensor. Anisotropic displacement parameters (U_{ij}) are defined as $\exp\{-2\pi^2[U_{11}\ h^2(a*)^2 + \ldots + 2U_{12}hk(a*)(b*) + \ldots]\}$.

Atom	*x*	*y*	*z*	U_{eq}	U_{11}	U_{22}	U_{33}	U_{23}	U_{13}	U_{12}
Bi1	0.0284(6)	0	0.0173(6)	0.0255(3)	0.0247(8)	0.0307(3)	0.0210(5)	0	−0.0028(4)	0
Mn1	0.0030(30)	0	0.4951(3)	0.0106(6)	0.0066(15)	0.0185(10)	0.0066(16)	0	−0.0041(10)	0
Mn2	0.4997(4)	0	0.5019(4)	0.0102(6)	0.014(2)	0.0101(9)	0.0069(13)	0	−0.0041(11)	0
Mn3	0.4955(2)	0	−0.0022(4)	0.0101(6)	0.0034(14)	0.0082(9)	0.0185(14)	0	−0.0049(10)	0
Mn4	0.2542(3)	0.7419(3)	0.2540(3)	0.0083(4)	0.0080(10)	0.0076(6)	0.0093(8)	−0.0020(7)	−0.0031(7)	−0.0030(8)
Mn5	0.2476(2)	0.74930(17)	0.74590(18)	0.0067(5)	0.0066(12)	0.0084(6)	0.0049(10)	−0.0016(5)	−0.0046(7)	0.0006(6)
O1	0.3366(19)	$\frac{1}{2}$	0.1827(18)	0.015(2)	0.006(5)	0.023(5)	0.015(6)	0	−0.007(4)	0
O2	0.1916(19)	0	0.6755(19)	0.017(2)	0.010(6)	0.023(5)	0.017(6)	0	−0.007(4)	0
O3	0.1742(18)	0	0.3031(18)	0.017(2)	0.004(5)	0.029(6)	0.017(6)	0	−0.001(4)	0
O4	0.825(2)	0	0.3094(19)	0.020(3)	0.012(6)	0.029(6)	0.017(6)	0	−0.010(5)	0
O5	0.4910(16)	0.8086(13)	0.3282(14)	0.0196(19)	0.016(4)	0.028(4)	0.015(4)	−0.015(3)	−0.006(3)	−0.006(4)
O6	0.3081(15)	0.8259(10)	−0.0105(14)	0.0192(15)	0.019(4)	0.016(4)	0.023(4)	0.001(3)	−0.009(3)	−0.001(3)
O7	0.0167(14)	0.6830(13)	0.1765(15)	0.0197(19)	0.009(4)	0.031(4)	0.019(4)	−0.010(3)	−0.006(3)	−0.010(4)
O8	0.6796(15)	0.1800(10)	0.0112(13)	0.0162(15)	0.017(4)	0.015(4)	0.016(4)	0.000(3)	−0.008(3)	−0.002(3)

TABLE II. Interatomic distances (Å).

Atoms	Distance	Atoms	Distance
Bi1-O3	2.392(14)	Mn3-O6	2×1.910(10)
Bi1-O6	2×2.481(9)	Mn3-O8	2×1.923(10)
Bi1-O7	2×2.631(10)		
Bi1-O5	2×2.697(10)	Mn4-O7	1.920(12)
Bi1-O4	2.706(13)	Mn4-O5	1.922(13)
Bi1-O2	2.872(15)	Mn4-O1	1.969(6)
Bi1-O1	2.874(14)	Mn4-O3	2.035(5)
Bi1-O8	2×2.945(11)	Mn4-O8	2.076(11)
		Mn4-O6	2.130(11)
Mn1-O1	1.907(14)		
Mn1-O4	1.916(16)	Mn5-O8	1.897(10)
Mn1-O2	1.943(16)	Mn5-O6	1.961(11)
Mn1-O3	1.956(13)	Mn5-O2	1.969(6)
		Mn5-O4	1.986(6)
Mn2-O7	2×1.887(11)	Mn5-O5	2.087(12)
Mn2-O5	2×1.925(10)	Mn5-O7	2.163(11)

CHARDIS,[17] indicates a 3+ oxidation state for all the Mn atoms.

The decrease in symmetry from the centrosymmetric space group $I2/m$, typical of other monoclinic $A^{3+}Mn_7O_{12}$ compounds, to Im in $BiMn_7O_{12}$ is mainly determined by the steric hindrance of the $6s^2$ lone pair of the Bi^{3+} ion. This typically produces a quite distorted coordination around the Bi atom, with the strongest bonds lying on the same side in order to accommodate the lone pair on the opposite one. As shown in Fig. 1(c), the Bi atom moves out from the center of the dodecahedral oxygen coordination determining an asymmetrical coordination. An electrical polarization of 7.33 $\mu C/cm^2$ at room temperature, mostly generated by the displacement of all the Bi atoms in a common direction, can be computed by a simple model as dipole moment for volume unit, suggesting the existence of ferroelectricity in $BiMn_7O_{12}$. This hypothesis is further supported by transmission electron microscope (TEM) investigations, performed on a Philips TECNAI F20 instrument operating at 200 kV, which show the presence in $BiMn_7O_{12}$ samples of twinning domains extending on a few tens of nanometers. They are pointed out by contrast variations in the bright-field and high-resolution electron microscopy (HREM) images, as reported in Figs. 2(a) and 2(b), respectively, taken in the $[11\bar{1}]$ zone axis. It can be noted that, in the image plane, the twinning boundaries in the direct space are normal to the 112 reciprocal lattice vector of the corresponding fast Fourier transform [Fig. 2(c)]. However the characteristic features of the contrast variation in the twin boundaries in Fig. 2(a) and the alternate sequence of sharp and blurred zones in the HREM image suggest the twinning boundaries to be inclined with respect to the zone axis. These considerations suggest that the twinning would occur in the (111) plane, a situation that is consistent with the inversion of the polar axis, namely, the shift of the Bi ions in opposite directions, in agreement with the anomalous elongation of the a.d.p.'s into the ac plane, when the structure is refined in the centrosymmetric $I2/m$ space group.

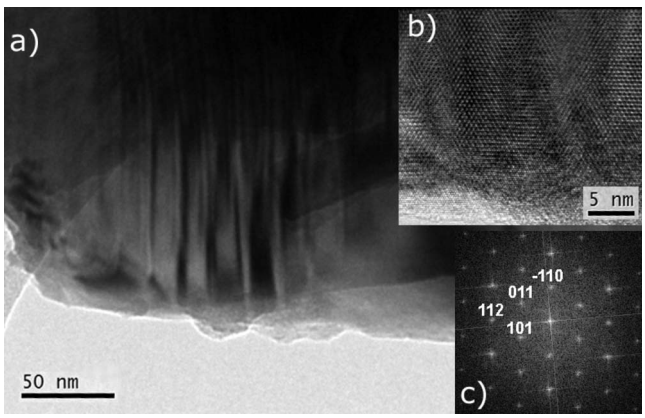

FIG. 2. Bright field (a) and high-resolution (b) TEM images taken in the $[11\bar{1}]$ zone axis showing the presence of twinning domains in a $BiMn_7O_{12}$ sample. Fast Fourier transform of the HREM image is shown in (c).

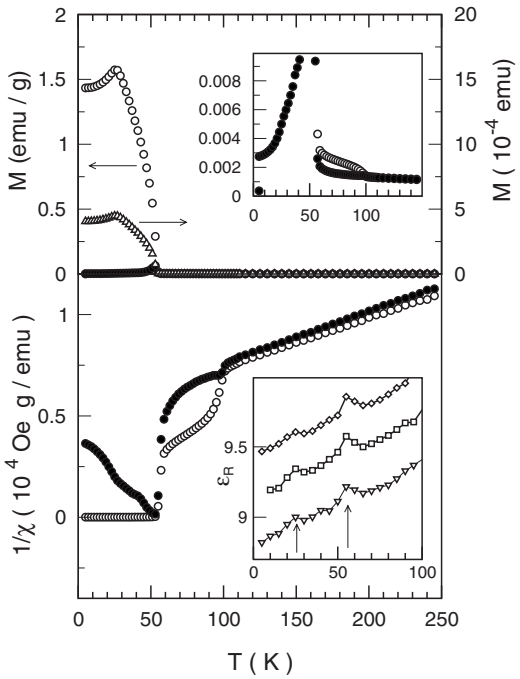

FIG. 3. ZFC (filled symbols) and FC (open symbols) dc magnetization curves (upper panel) and inverse susceptibility (lower panel) in applied magnetic field $H=10$ Oe: (○) and (●) polycrystal; (△) single crystal. Upper inset: secondary transition in the magnetization curve at $T \approx 100$ K. Lower inset: dielectric constant measured at selected frequencies: (◇) 3, (□) 125, and (▽) 500 kHz.

The magnetic properties of $BiMn_7O_{12}$ have been studied using a superconducting quantum interference device (SQUID) magnetometer. The measurements yield similar results for single-crystal and polycrystalline samples; however the signal given by single crystals is very weak in the paramagnetic region, approaching the instrumental sensitivity. The zero-field-cooled (ZFC) and field-cooled (FC) dc magnetization curves in applied magnetic field $H=10$ Oe are reported in Fig. 3 (upper panel), where a sharp transition to

antiferromagnetic regime at $T_c \approx 50$ K can be seen. The antiferromagnetic nature of the ordered phase is more clear looking at the inverse susceptibility shown in Fig. 3 (lower panel), where one can also estimate the Curie-Weiss temperature $\theta \approx 206$ K. The anomaly at $T \approx 100$ K could be ascribed to the possible presence of $BiMnO_3$ impurities, whose monoclinic phase undergoes a ferromagnetic transition at $T_c = 99$ K (Ref. 18) recoverable in an amplified view of the magnetization curve (inset of Fig. 3). From the magnetization of $BiMnO_3$ (Ref. 19) one can assess that the impurity is less than 1%. The sharp drop of the inverse susceptibility at T_c has the shape usually observed in stoichiometrically pure Dzyaloshinskii-Moriya (DM) compounds.[20,21] It is worth to remark on that a similar behavior is also observed in the structurally related compounds $PrMn_7O_{12}$ (Ref. 22) and $LaMn_7O_{12}$,[14] while it is absent in the simple perovskite $BiMnO_3$. This can be easily understood because the DM interaction, which is an antisymmetric exchange interaction between two spins $\mathbf{S_i}$ and $\mathbf{S_j}$ of the form $\mathcal{D} \cdot (\mathbf{S_i} \times \mathbf{S_j})$ arising from the spin-orbit coupling, gives rise to nonzero net result only when certain symmetry constrains are fulfilled; namely, the midpoint between $\mathbf{S_i}$ and $\mathbf{S_j}$ must not be a center of inversion. This condition is fulfilled because of the sizeable tilting of the MnO_6 octahedra in $BiMn_7O_{12}$, contrary to the case of $BiMnO_3$. A detailed study of the magnetic structure by neutron diffraction is in progress. The slope of the inverse susceptibility yields ≈ 6 μ_B/Mn, while the expected value for Mn^{3+} ions would be 4.9 μ_B/Mn. The antiferromagnetic peak at 26 K corresponds to the ordering of the Mn ions in the planarly coordinated A' sites.

The dielectric constant was measured by applying mica linings to the sample in order to remove the extrinsic contribution coming from contact junctions.[23] The results at selected frequencies are reported in Fig. 3 (lower inset) and show two distinct anomalies corresponding to the magnetic transitions, suggesting therefore a coupling between magnetic and dielectric properties of $BiMn_7O_{12}$.

In conclusion, we have synthesized by HP/HT $BiMn_7O_{12}$, a member of the family of manganites with quadruple-perovskite structure. Detailed structural characterization carried out by single-crystal x-ray diffraction yields the definition of a noncentrosymmetric space group (*Im*). This feature is originated by the stereochemical effect induced by the presence of Bi^{3+} ions, which in virtue of the $6s^2$ lone pair induces an asymmetrical coordination of the oxygen neighbors, leading to a permanent electrical dipole moment, allowing ferroelectricity in this material. Magnetic characterization points out, in agreement with isostructural compounds, the presence of antiferromagnetic transitions at 50 and 26 K corresponding to the ordering of the B and A' sites, respectively. Measurements of dielectric constant show also coupling between magnetic and dielectric degrees of freedom. The coexistence of the two ferroic orders makes $BiMn_7O_{12}$ a promising multiferroic material, with interesting evidence of magnetodielectric behavior.

The authors wish to express their gratitude to G. André, F. Bourée, A. Gauzzi, G. Rousse, A. Prodi, and F. Licci for fruitful discussions and to T. Besagni for XRD. A few high-pressure experiments of $BiMn_7O_{12}$ were performed at the Bayerisches Geoinstitut at Bayreuth (Germany) under the EU "Research Infrastructures: Transnational Access" Programme [Contract No. 505320 (RITA)-High Pressure].

*Corresponding author; francesco.mezzadri@nemo.unipr.it

[1] H. Schmid, Ferroelectrics **162**, 317 (1994).
[2] Ce-Wen Nan *et al.*, J. Appl. Phys. **103**, 031101 (2008).
[3] T. Kimura *et al.*, Nature (London) **426**, 55 (2003).
[4] G. R. Blake *et al.*, Phys. Rev. B **71**, 214402 (2005).
[5] N. Ikeda *et al.*, Nature (London) **436**, 1136 (2005).
[6] J. Wang *et al.*, Science **299**, 1719 (2003).
[7] C. Ederer and N. A. Spaldin, Phys. Rev. B **74**, 024102 (2006).
[8] T. Rudolf *et al.*, Phys. Rev. B **75**, 052410 (2007).
[9] H. D. Megaw, Acta Crystallogr. **5**, 739 (1952).
[10] D. J. Singh, Phys. Rev. B **73**, 094102 (2006).
[11] M. Marezio *et al.*, J. Solid State Chem. **6**, 16 (1973).
[12] B. Bochu *et al.*, J. Solid State Chem. **29**, 291 (1979).
[13] A. Prodi *et al.*, Nature Mater. **3**, 48 (2004).
[14] A. Prodi *et al.*, Phys. Rev. B **79**, 085105 (2009).
[15] G. M. Sheldrick, *SHELX97, Program for Crystal Structure Refinement* (University of Goettingen, Germany, 1997).
[16] Michael N. Burnett and Carroll K. Johnson, "ORTEP-III: Oak Ridge Thermal Ellipsoid Plot Program for Crystal Structure Illustrations," Oak Ridge National Laboratory Report No. ORNL-6895, 1996 (unpublished).
[17] M. Nespolo *et al.*, Acta Crystallogr. **B55**, 902 (1999).
[18] E. Montanari *et al.*, Chem. Mater. **17**, 6457 (2005).
[19] E. Montanari *et al.*, Phys. Rev. B **75**, 220101(R) (2007).
[20] J. Topfer and J. B. Goodenough, J. Solid State Chem. **130**, 117 (1997).
[21] J. Hemberger *et al.*, Phys. Rev. B **75**, 035118 (2007).
[22] F. Mezzadri *et al.*, Phys. Rev. B **79**, 014420 (2009).
[23] R. Cabassi *et al.*, Phys. Rev. B **74**, 045212 (2006).